Chemical Science

RSC Publishing

EDGE ARTICLE

View Article Online
View Journal | View Issue

Published on 23 July 2013. Downloaded by Michigan State University on 21/01/2016 19:52:01.

Cite this: *Chem. Sci.*, 2013, **4**, 3965

Seeing through solvent effects using molecular balances†

Ioulia K. Mati, Catherine Adam and Scott L. Cockroft‡*

Received 24th June 2013
Accepted 22nd July 2013

DOI: 10.1039/c3sc51764k

www.rsc.org/chemicalscience

The study of molecular interactions is often complicated by solvent effects. Here we have used a series of 11 synthetic molecular balances to measure solvent and substituent effects on the positions of conformational equilibria in 13 different solvents. Despite the simplicity of the model system, surprisingly complicated behaviour was seen to emerge from the interplay of conformational, intramolecular and solvent effects. Nonetheless, 138 experimental conformational free energies were analysed using a simple solvent model, which was able to account for both the major and more unusual patterns observed. The success of the solvent model can be attributed to its ability to facilitate consideration of individual intramolecular and solute–solvent interactions, as confirmed by comparison with NMR chemical shifts and DFT calculations. The approach provides a means of dissecting electrostatic and solvent effects to reveal pseudo gas-phase behaviour from experimental data obtained in solution. For example, the method facilitated the identification of an unexpected, but highly favourable C=O···NO_2 interaction worth up to 3.6 kJ mol^{-1}, which was shown not to be driven by solvent effects.

Introduction

Non-covalent interactions underpin chemistry and biology. They determine the stereochemical outcomes of reactions,[1–3] ligand–receptor binding,[4–7] and the structure and function of proteins, nucleic acids[8,9] and other supramolecular architectures.[10,11] However, few experimental approaches exist for dissecting individual contributions to the complicated arrays of interactions and solvent effects governing molecular behaviour.[12–17]

Molecular balances, pioneered by Ōki,[18] and Wilcox,[19,20] are a useful platform for the study of non-covalent interactions since the positions of conformational equilibria are determined by intramolecular interactions and solvent effects.[21] Such systems have been used to measure a whole range of interactions including aromatic interactions,[15–31] orthogonal dipolar interactions,[32–34] and deuterium isotope effects.[35] Molecular balances present a number of advantages for the study of molecular recognition phenomena. Firstly, the geometries of intramolecular interactions are typically better defined than in supramolecular complexes. Secondly, they enable the measurement of very weak non-covalent interactions since conformational equilibria are sensitive to small free energy differences, while the intramolecular approach evades the significant entropic costs associated with bimolecular complexation.[36,37] Finally, where variation of the solvent often adversely affects solubility and binding constants in supramolecular complexes, thermodynamic data can be extracted from molecular balances in any solvent provided that it is sufficiently soluble for an NMR spectrum to be obtained.

Even though molecular balances are inherently suited to the systematic study of solvent effects, they have rarely been used to examine more than a handful of solvents.[15–17,23–25] Here we have employed a series of simple molecular balances as a quantitative probe of electronic effects on the position of conformational equilibria in a wide range of solvents (Fig. 1 and 2). Rotation about the formyl C–N bond in these balances was measured as 75.1 kJ mol^{-1} (Fig. S21†), which means that these balances exist in equilibrium between spectroscopically-distinct conformers on the NMR timescale. Since the chemical shift of the fluorine atom

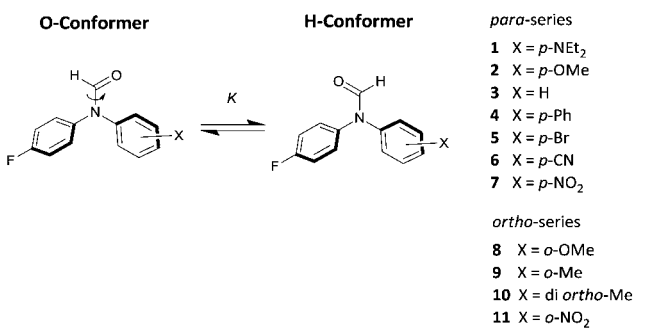

Fig. 1 Conformational equilibrium for the formamide balances synthesised in this study.

EaStCHEM School of Chemistry, University of Edinburgh, King's Buildings, West Mains Road, Edinburgh, EH9 3JJ, UK. E-mail: scott.cockroft@ed.ac.uk; Tel: +44 (0) 131 650 4758

† Electronic supplementary information (ESI) available: Additional data, and experimental and computational methods. See DOI: 10.1039/c3sc51764k

‡ Celebrating 300 years of Chemistry at Edinburgh.

Published on 23 July 2013. Downloaded by Michigan State University on 21/01/2016 19:52:01.

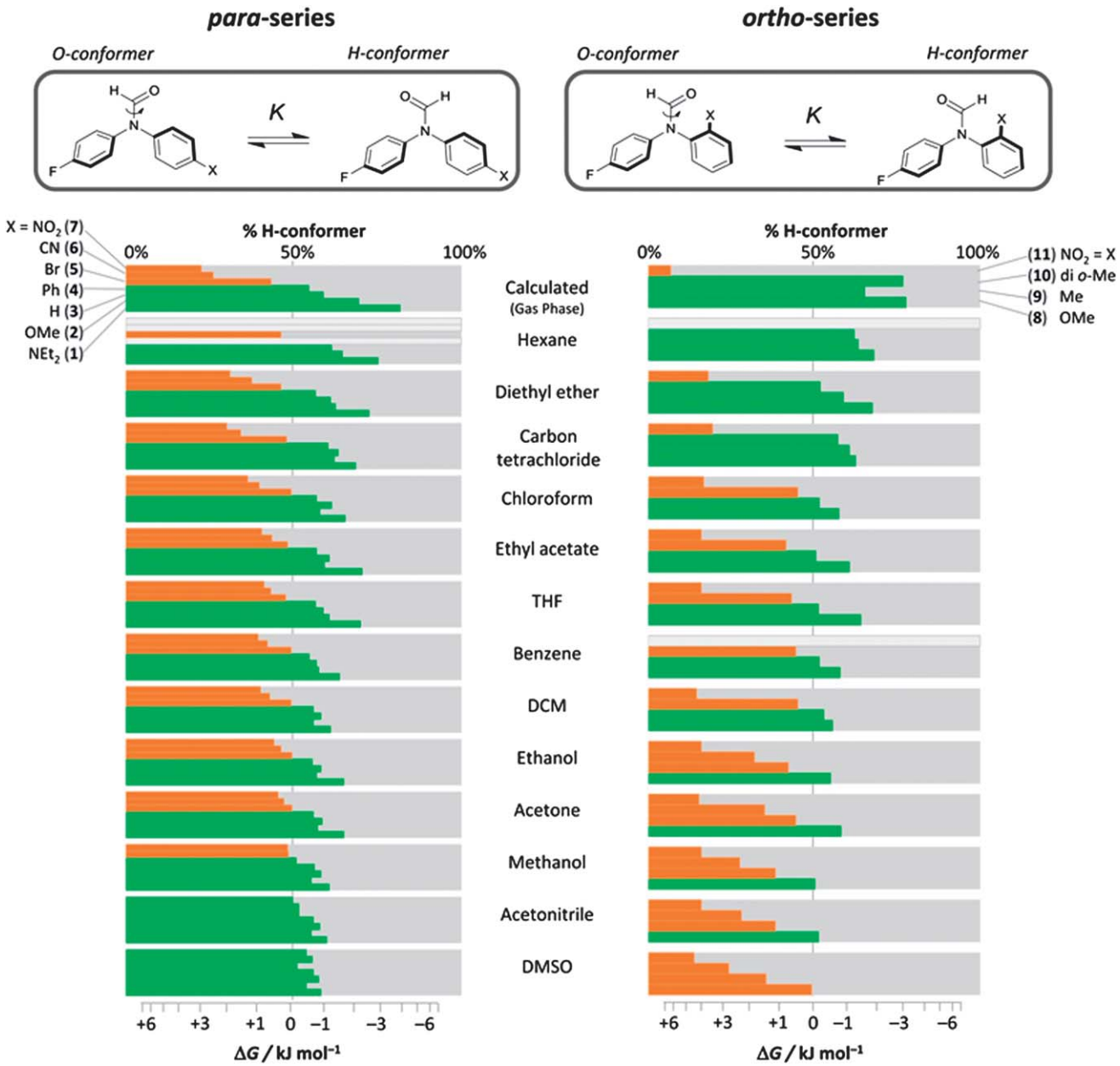

Fig. 2 Percentages of H conformers and conformational free energies of balances **1–11** determined in 13 solvents and calculated by B3LYP/6-31G* in the gas-phase. Orange bars indicate positive ΔG values (O-conformer preferred) and green bars indicate negative ΔG values (H-conformer preferred). The missing values in hexane indicated by the light grey bars correspond to points where the balances were insufficiently soluble to obtain data, while the missing data for balance **11** in benzene was due to peak overlap in the NMR spectrum. Tabulated data are provided in Table S1† and also indicate whether deuterated or non-deuterated solvents were used.

in the balances is sensitive to the rotational isomerisation of the formyl group, ^{19}F-NMR was used to determine the conformational equilibrium constants (K) in a range of readily accessible solvents. 138 conformational free energy differences were determined for 11 molecular balances in 13 different solvents (using $\Delta G = -RT\ln K$). Despite the apparent simplicity of these balances, complicated behaviour was revealed as the substituents and solvents were varied (Table 1 and Fig. 2).

Thus, these data were analysed using a simple solvation model to see whether it could provide any insight into the individual interactions in governing the observed behaviour.

Results & discussion

Conformational equilibrium constants were measured in the 13 solvents shown in Fig. 2 and calculated in the gas-phase using B3LYP/6-31G* (Table S1†). The major trends in the conformational energies of the *para*-substituted balances indicate that the equilibrium is driven by electronic substituent effects in apolar solvents, with the formyl oxygen preferring to lie over the least electron-rich ring. Accordingly, the balances generally follow the same pattern of energies; balances bearing X substituents that are more electron donating than fluorine (**1**, **2**,

This journal is © The Royal Society of Chemistry 2013

Published on 23 July 2013. Downloaded by Michigan State University on 21/01/2016 19:52:01.

Table 1 ΔE, $\Delta\alpha$ and $\Delta\beta$ determined for balances **1–11** by fitting experimental conformational free energies to the model shown in Fig. 3

		ΔE/kJ mol^{-1}	$\Delta\alpha$	$\Delta\beta$
1	*p*-NEt_2	−2.8 ± 0.4	0 ± <0.1	+0.6 ± 0.2
2	*p*-OMe	−1.6 ± 0.2	0 ± <0.1	+0.3 ± 0.1
3	H	−1.2 ± 0.2	0 ± <0.1	+0.1 ± <0.1
4	*p*-Ph	−0.8 ± 0.1	0 ± <0.1	0 ± <0.1
5	*p*-Br	+0.5 ± 0.1	0 ± <0.1	−0.2 ± <0.1
6	*p*-CN	+1.9 ± 0.4	−0.2 ± <0.1	−0.4 ± 0.3
7	*p*-NO_2	+2.6 ± 0.5	−0.2 ± <0.1	−0.5 ± 0.2
8	*o*-OMe	−2.3 ± 0.3	+0.1 ± <0.1	+0.8 ± 0.3
9	*o*-Me	−2.1 ± 0.4	+0.2 ± <0.1	+0.8 ± 0.2
10	di-*o*-Me	−2.0 ± 0.5	+0.3 ± <0.1	+1.0 ± 0.3
11	*o*-NO_2	+3.6 ± 0.3	+0.1 ± <0.1	+0.2 ± 0.1

3, **4**, X = NEt_2 to Ph) prefer the H-conformer (ΔG < 0), while balances with electron-withdrawing groups (**5**, **6**, **7**, X = Br, CN, NO_2) prefer the O-conformer (ΔG > 0). The larger the electronic difference between the F-substituted and the X-substituted ring, the greater the magnitude of ΔG. The sensitivity of each balance to the electronic effects of the substituents is also highly dependent on the solvent. Apolar solvents have the largest conformational free energy differences, and are most similar to the calculated gas-phase energies (*e.g.* ΔG_{exp} = −2.4 and +2.0 kJ mol^{-1} for X = NEt_2 and NO_2, respectively in diethyl ether). As the solvents become more polar the energies digress further from the calculated gas-phase free energy and become closer to zero (*e.g.* −0.8 and −0.4 kJ mol^{-1} for X = NEt_2 and NO_2 in DMSO).

While the major patterns in the *para*-substituted balances are easily rationalised, not all of the trends are so easily explained, particularly for the *ortho*-substituted balances (Fig. 2, right column):

(i) The *para*-substituted balances bearing electron-withdrawing groups prefer the H-conformer as solvent polarity increases, which cannot be explained by gas-phase electrostatic effects. In the *ortho*-substituted balances the trend is reversed and the preference for the O-conformer increases with solvent polarity.

(ii) The *ortho*-Me, di *ortho*-Me and *ortho*-OMe balances are more sensitive to solvent effects than any of the *para*-substituted balances (including those bearing polar substituents such as NO_2 and CN).

(iii) The *ortho*-NO_2 balance is relatively insensitive to the modulating effects of the solvent and has the most extreme ΔG values ranging between +3.5 and +4.5 kJ mol^{-1}. This contrasts with the behaviour of the other *ortho*-substituted balances and the *para*-NO_2 balance, which are very sensitive to solvent effects.

In spite of the simplicity of the model system, it is difficult to rationalise these patterns without further analysis, other than to say that intramolecular electrostatic and solvent effects must both play a role in determining the conformational preferences. Thus, the challenge arises as to whether it is possible to dissect-out the individual factors contributing to the observed conformational free energies.

Dissecting solvent effects using a simple solvent model

Hunter's α/β hydrogen-bond model has been shown to account for[15] and predict[16] solvent effects on the conformational free energies of Wilcox molecular torsion balances, in addition to edge-to-face aromatic interactions in supramolecular complexes[16] and hydrogen-bonding interactions in many different solvents and solvent mixtures.[13,38] Thus, we were curious to ascertain whether a simple α/β solvation model would be able to account for the large volume of data obtained in the present study (comprising 138 experimental free energy measurements obtained for 11 different molecular balances in 13 solvents).

We reasoned that the conformational free energies would be governed by the intramolecular electrostatic and steric differences between the O- and the H-conformers (encoded by ΔE), and the global differences in the hydrogen-bond donor and acceptor constants of each conformer ($\Delta\alpha$ and $\Delta\beta$), as represented in Fig. 3. This schematic representation only shows single hydrogen-bond donor and acceptor sites, but in reality the $\Delta\alpha$ and $\Delta\beta$ terms will be determined by the Boltzmann average of all possible solvation sites on each balance.

The experimental conformational free energies of each balance as the α_s and β_s hydrogen-bond donor and acceptor constants were varied (by changing the solvent) were fitted to the equation shown in Fig. 3 using a least squares linear regression. Overall, the fitting gave an R^2 = 0.96 between the predicted ($\Delta G_{\alpha/\beta\ model}$) and the experimental free energies (ΔG_{exp}) for all balances and solvents examined (Fig. 4).[39] Notably, this fitting included all of the initially surprising results summarised in points (i) to (iii) above, but nonetheless, these ΔG values were as well predicted as the balances with the more easily rationalised conformational preferences.

The fitting process provides values of ΔE, $\Delta\alpha$ and $\Delta\beta$ for each of the balances examined, which provide insight into the individual interactions contributing to the experimental

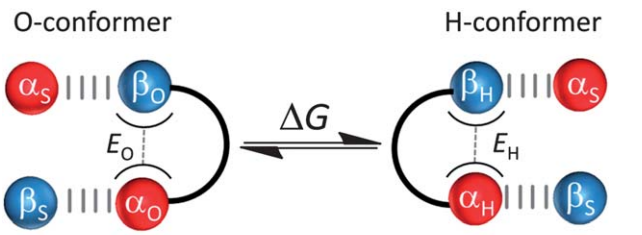

$$\Delta G = E_H - E_O + \alpha_S\beta_O + \beta_S\alpha_O - \beta_S\alpha_H - \alpha_S\beta_H$$
$$= E_H - E_O + \alpha_S(\beta_O - \beta_H) + \beta_S(\alpha_O - \alpha_H)$$
$$= \Delta E + \beta_S\Delta\alpha + \alpha_S\Delta\beta$$

Fig. 3 A simple solvation model showing the individual terms contributing to conformational free energies (where solvophobic effects are negligible). E_O and E_H correspond to the intramolecular steric and electronic effects in the O- and H-conformers respectively, and α_s, α_O, α_H, β_s, β_O, and β_H are the global hydrogen-bond donor (α) and acceptor constants (β) of the solvent, and the O- and the H-conformers respectively.

Published on 23 July 2013. Downloaded by Michigan State University on 21/01/2016 19:52:01.

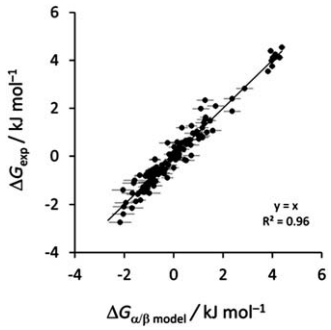

Fig. 4 Correlation between experimentally determined conformational free energies (ΔG_{exp}) and corresponding values predicted from the α/β model for balances **1–11** in 13 different solvents.

conformational free energies (Table 1). The high-quality correlation between the determined ΔE values and gas-phase conformational free energy differences calculated using B3LYP/6-31G* (ΔG_{DFT}, Fig. 5a, S5–11 and Table S5†), confirm that the ΔE term corresponds to the intramolecular contributions to ΔG_{exp}. Notably, simply averaging the ΔG_{exp} values for each balance across all solvents examined resulted in a comparatively poorer correlation against ΔG_{DFT}, particularly for the *ortho*-substituted balances, which highlights the advantage of the energetic dissection facilitated by the α/β solvation model (Fig. S3a†). Consistent with a dominant electrostatic component, balances bearing electron-donating groups have negative ΔE, while those with electron-withdrawing substituents have positive ΔE values. The electrostatic component of ΔE is revealed in the correlations with both σ_m Hammett substituent constants (Fig. 5b), and electrostatic potentials taken over the corresponding carbon atoms positioned *meta* to X substituents in the *para*-substituent series of balances (ESP_{meta}, Fig. 5c). Although high correlation coefficients are also seen in correlations of ΔG_{exp} values averaged across all solvents for the *para*-substituted balances, these graphs have significantly shallower gradients than those shown in Fig. 5b and c (Fig. S3b and c†). The differences in the gradients arise because the damping effects of the solvent are simply averaged in the ΔG_{ave} plots shown in Fig. S3,† while the greater variation of the ΔE values (obtained by application of the α/β-model) is consistent with solvent effects being dissected away to reveal the pseudo-gas-phase behaviour resulting from intramolecular interactions. Overall, Fig. 5 shows that the ΔE term follows the expected intrinsic stability trends (without the influence of solvent).

In contrast to the solvent-independent ΔE values, the energetic effects of $\Delta\alpha$ and $\Delta\beta$ are modulated by the solvent (*via* the $\beta_s\Delta\alpha$ and $\alpha_s\Delta\beta$ terms, as shown in Fig. 3). In general, more polar solvents with larger α_s and β_s constants decrease ΔG differences between conformers because the sign of the $\Delta\alpha$ and $\Delta\beta$ terms oppose that of the ΔE term. The $\Delta\beta$ term varies more than $\Delta\alpha$ across the series of balances examined, and is consistent with solvation of the highly polar formyl oxygen atom having a large influence on the position of the conformational equilibrium (see electrostatic surface potentials in Fig. S5–S11†).

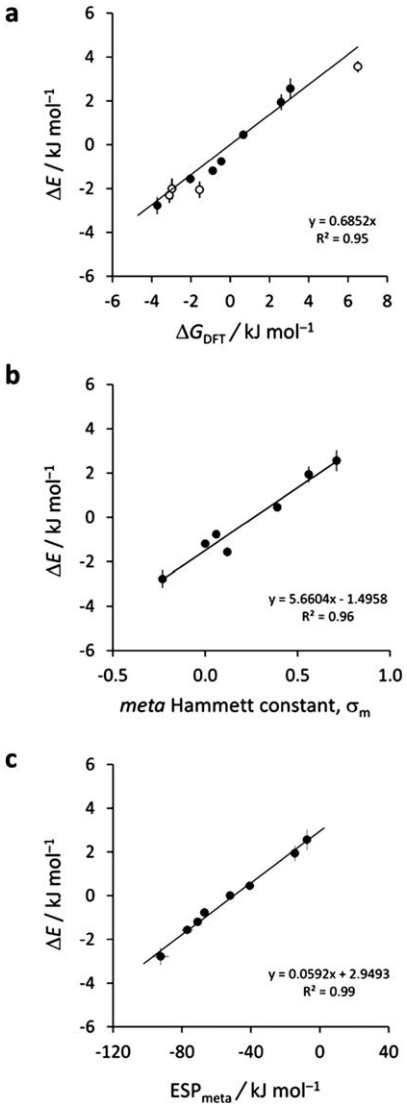

Fig. 5 Correlation between the solvent-independent ΔE term dissected using the model in Fig. 3 and (a) gas-phase conformational free energies ΔG_{DFT} calculated using B3LYP/6-31G*, (b) *meta* Hammett substituent constants for the *para*-X substituents and, (c) the electrostatic potentials on the molecular surface over the carbon atoms positioned *meta* to the *para* X-substituent calculated using B3LYP/6-31G*. Data for the *para*-substituted balances **1–7** are indicated with black circles, and the *ortho*-substituted balances **8–11** by hollow circles, and is provided in Table S4.†

Furthermore, the calculated electrostatic potential minima of these oxygen atoms correlate well with $\Delta\beta$ values determined for all 11 molecular balances in the O- and H-conformers (Fig. 6). Looking beyond the major trends, closer examination of the $\Delta\alpha$ and $\Delta\beta$ terms provides and explanation for the more unusual experimental observations outlined in points (i) to (iii) above. In point (i), it was noted that the *p*-EWG balances displayed a preference for the H-conformer as solvent polarity increased, while this behaviour was not observed in the *p*-EDG balances. This solvent-dependent switching of conformers whilst the substituent remains constant indicates that solvent effects in the most polar solvents must dominate over intramolecular interactions.

 This journal is © The Royal Society of Chemistry 2013

Published on 23 July 2013. Downloaded by Michigan State University on 21/01/2016 19:52:01.

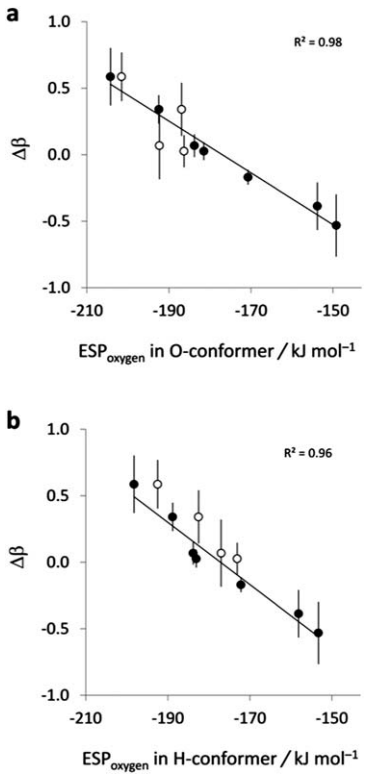

Fig. 6 (a) Correlation between the $\Delta\beta$ term dissected using the model in Fig. 3 and the electrostatic potential minima over the formyl oxygen for balances **1–11** in the O- and H-conformers. Electrostatic potentials were calculated using B3LYP/6-31G*. The *para*-substituted balances **1–7** are indicated with black circles, and the *ortho*-substituted balances **8–11** by hollow circles. The corresponding data is provided in Table S5.†

Taking the example of balance 7, where X = NO_2; fitting the experimental data to the model depicted in Fig. 3 gave ΔE = +2.6 kJ mol^{-1}, $\Delta\beta = -0.5$ and $\Delta\alpha = -0.2$. These solvent-dependent $\Delta\beta$ and $\Delta\alpha$ values are consistent with a possible role for solvent interactions competing with intramolecular interactions between the formyl oxygen and the protons on the edges of the aromatic rings. Although NMR data indicate that the *para*-substituted aromatic rings are freely rotating in solution, the average conformation of the rings may vary as the substituents are varied such that interactions between the formyl oxygen and the aromatic protons may influence the position of the conformational equilibrium (in addition to the differences in the electrostatic potentials of the faces of the aromatic rings).

Support for this hypothesis can be found in the crystal structures of related compounds (Fig. S12†), and the minimised calculated structures of molecular balances **1–11** (Fig. S5–S11†). The dihedral angles of these structures indicate that aromatic rings bearing EWGs lie closer to the plane of the adjacent amide group, whilst rings bearing EDGs are twisted further from the plane of the amide (Table S6† and Fig. 8). Rings bearing electron-withdrawing X-substituents could be expected to favour a more planar average conformation that allows conjugation between the EWG and the lone pair electrons of the formamide nitrogen, particularly when the proposed intramolecular interaction between the formyl oxygen and the edge of the polar aromatic can occur.

Evidence for intramolecular interactions between the formyl oxygen and the edges of the aromatic rings is provided by experimental NMR data (Fig. 8). In the balances featuring *p*-EWGs, the chemical shift of the proton implicated as being involved in the intramolecular hydrogen-bond is up to 0.3 ppm higher in the O-conformer compared to the H-conformer, while the adjacent protons, which are not involved in hydrogen-bonding interactions change by less than 0.04 ppm (Fig. 8a and Table S8†). Meanwhile the chemical shift trend is reversed for the *p*-EDG balances indicating that in these cases a weak intramolecular hydrogen bond is formed in the H-conformer rather than the O-conformer (Fig. 8b). These chemical shifts are small, but nonetheless significant and are consistent with the weak nature of these interactions and rapid rotation of the aromatic rings about the aromatic C–N bond.

It follows that solvents with a strong hydrogen-bond acceptor constant such as DMSO will compete with the formyl oxygen in the binding of the polar aromatic protons, driving the equilibrium towards the H-conformer ($\Delta\alpha$ and $\Delta\beta$ = −ve, Fig. 7a). In contrast, the formyl oxygen interaction with the edge of the fluorine-substituted ring will be more favourable than the equivalent interactions with a ring bearing an EDG. Thus, when X is an EDG, a polar solvent competes most with the intramolecular interactions involving the F-substituted ring, driving the conformation towards the O-conformer rather than the H-conformer ($\Delta\beta > 0$, Fig. 7b). However, because the edge of a fluorine-substituted ring is less polar than those where X = NO_2

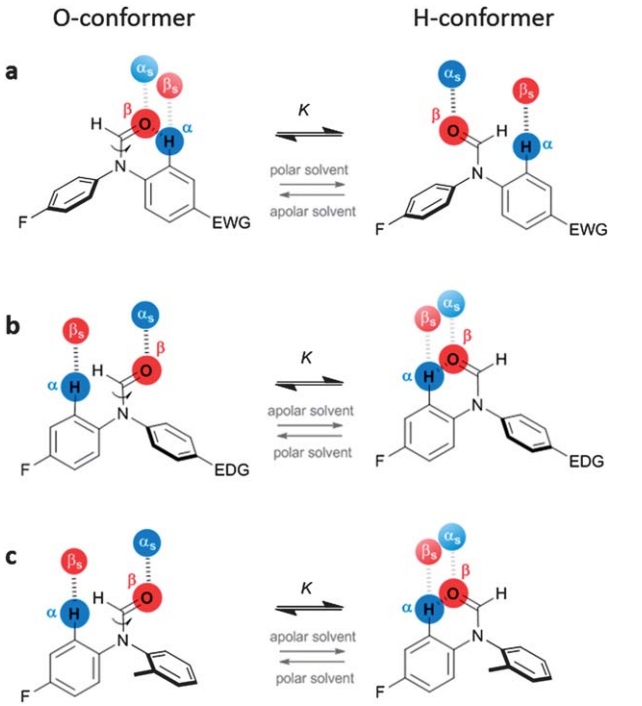

Fig. 7 Proposed intramolecular and solvent interactions contributing to the conformational free energy differences in balances **1–11**. EDG = electron-donating group, EWG = electron-withdrawing group.

Published on 23 July 2013. Downloaded by Michigan State University on 21/01/2016 19:52:01.

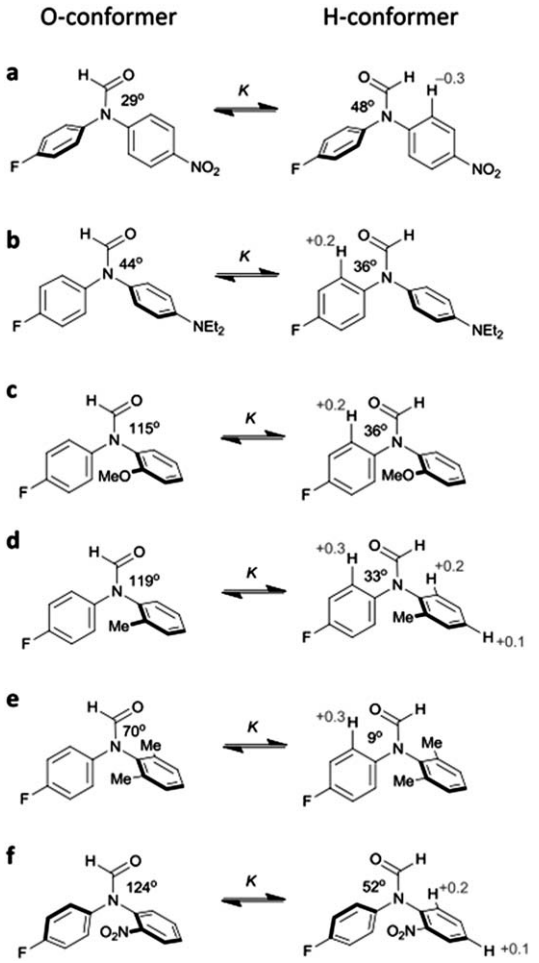

Fig. 8 Experimental changes in proton chemical shift on going from the O-conformer to the H-conformer in $CDCl_3$ (grey text), and dihedral angles between the CH-aromatic plane and the formamide plane (C_{ortho}–C_{ipso}–N_{amide}–C_{amide}) from minimised conformer structures calculated using B3LYP/6-31G* (Fig. S5–S11†). Only chemical shifts greater than ±0.1 ppm are shown, and a complete table of chemical shifts is provided in Tables S7 and S8.†

or CN, then even solvation by DMSO is not sufficient to fully overcome the intramolecular interactions encoded by ΔE and the H-conformer is still marginally preferred ($\Delta\alpha \approx 0$, Fig. 2).

With reference to point (ii) above, the sensitivity of the *ortho*-Me, di *ortho*-Me and *ortho*-OMe balances to variation of the solvent can also be explained within the framework of solvent competing with intramolecular electrostatic interactions. Calculated minimised structures show that *ortho*-substituents twist the substituted ring out of the plane of the formamide (dihedral angles in Fig. 8c–f and S5–S11†). The twist of the *ortho*-substituted ring means that a formyl oxygen-aromatic edge interaction can only be formed with the edge of the fluorine-substituted ring (Fig. 7c). Accordingly, the chemical shifts of the proton *meta* to the fluorine are seen to shift 0.2–0.3 ppm on going from the O- to the H-conformer (Fig. 8c–e). In contrast, chemical shifts on all protons on the *ortho*-X-substituted rings either change little between conformers (X = *o*-OMe and di-*o*-Me, Fig. 8c and e), or are shifted in the opposite direction to that consistent with formation of an internal hydrogen-bond in the H-conformer. Since such shifts are seen in both the *ortho* and *para* protons in the X = *o*-Me (and *o*-NO_2) balances, this can be attributed to a general decrease in the electron density of the X-substituted ring arising from removal of the electron-rich formyl oxygen from above the ring on going from the O- to the H-conformer (Fig. 8d and f). Thus, according to the solvation model depicted in Fig. 7c, even solvents that are weakly solvating are able to break the weak intramolecular interactions with the F-substituted ring and drive the balances towards the readily solvated O-conformer (in which even less intramolecular competition exists). This effect manifests itself in the positive $\Delta\alpha$ and $\Delta\beta$ terms listed in Table 1, which are significantly more positive than those encountered in *para*-series.

Finally, with regards to the relative insensitivity of the *o*-NO_2 balance to solvent effects (point (iii) above), application of the solvent model shown in Fig. 3 reveals ΔE = +3.6 kJ mol^{-1}, $\Delta\alpha$ = +0.1 and $\Delta\beta$ = +0.1, indicating that the strong preference for the O-conformer is driven almost entirely by intramolecular interactions. In contrast to the other *ortho*-substituted balances investigated, both NMR chemical shifts and minimised geometry calculations are consistent with a minimal influence of solvent-sensitive interactions between the formyl oxygen and the edges of either the F- or the *o*-NO_2 substituted rings (Fig. 8f and Tables S7 and S8†). Instead, the minimised structure of the highly favoured O-conformation reveals that the oxygen of the formyl group is positioned above the δ-positive nitrogen atom and adjacent aromatic carbon (Fig. 9). This contact may be the driving force for the strong preference for the O-conformer in solution and calculated in the gas-phase, and appears similar to other favourable oxygen-carbonyl interactions that have been previously reported.[32–34,40,41] Notably, the dissected ΔE value is +3.6 ± 0.3 kJ mol^{-1} (towards the O-conformer hosting the C=O···NO_2 interaction), which is within error of the estimated strength of the C=O···NO_2 interaction of −3.3 kJ mol^{-1} obtained by taking the average of the difference between ΔG_{exp} for the *p*-NO_2 and *o*-NO_2 balances in all of the solvents examined (to control for background electronic and solvent effects).

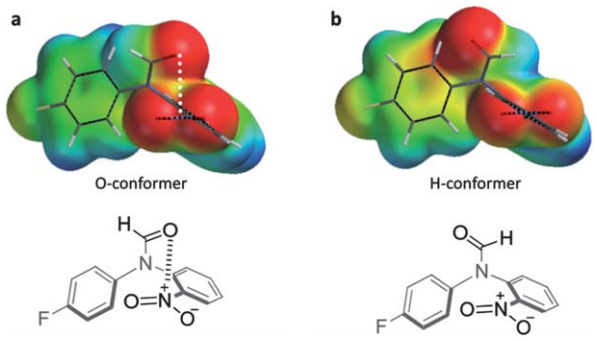

Fig. 9 Electrostatic surface potentials and minimised geometries of the *ortho*-NO_2 balance (**11**) in the O- and H-conformations showing alignment and contact of the formamide oxygen with the δ-positive nitrogen of the nitro group. The structures and electrostatic potentials were calculated using B3LYP/6-31G*, and electrostatic potentials are scaled from −125 kJ mol^{-1} (red) to +125 kJ mol^{-1} (blue).

This journal is © The Royal Society of Chemistry 2013

Published on 23 July 2013. Downloaded by Michigan State University on 21/01/2016 19:52:01.

Conclusions

This study demonstrates how complicated behaviour may arise in seemingly simple chemical systems as a result of the interplay of conformational, intramolecular and solvent effects. Despite these complexities, the application of a simple solvation model was able to provide insight into the individual interactions governing the behaviour observed in 11 different molecular balances in 13 different solvents. The approach allowed the main energy contributions governing conformer populations to be dissected into three main constituents – an intramolecular component, ΔE, and solvent-dependent hydrogen-bond donor and acceptor components, $\Delta\alpha$ and $\Delta\beta$. The ΔE term was found to correlate with calculated free energy differences between conformers and to reveal intramolecular interactions that could be attributed mostly to the electronic effects of the substituents. The hypotheses describing the experimental trends were further supported by NMR chemical shift data and calculated electrostatic potentials. An unanticipated, yet strikingly favourable C═O···NO_2 interaction was identified in one of the molecular balances investigated, which was determined to be driven almost entirely by direct intramolecular interactions and not by solvent effects. The approach may provide a useful platform testing theoretical models of solvation and for revealing the underlying principles influencing molecular recognition phenomena and the behaviour of other systems. It will be interesting to see the limitations of the simple method employed here, and whether more sophisticated solvation models[42] will be better suited to tackling the challenges presented by larger chemical systems.

Acknowledgements

We thank the School of Chemistry and Pfizer Ltd for funding PhD studentships for IKM and CA respectively.

Notes and references

1 R. R. Knowles and E. N. Jacobsen, *Proc. Natl. Acad. Sci. U. S. A.*, 2010, **107**, 20678–20685.
2 J. Meeuwissen and J. N. H. Reek, *Nat. Chem.*, 2010, **2**, 615–621.
3 A. G. Doyle and E. N. Jacobsen, *Chem. Rev.*, 2007, **107**, 5713–5743.
4 C. S. Chow and F. M. Bogdan, *Chem. Rev.*, 1997, **97**, 1489–1514.
5 H.-J. Böhm and G. Klebe, *Angew. Chem., Int. Ed. Engl.*, 1996, **35**, 2588–2614.
6 C. Bissantz, B. Kuhn and M. Stahl, *J. Med. Chem.*, 2010, **53**, 5061–5084.
7 D. H. Williams, E. Stephens, D. P. O'Brien and M. Zhou, *Angew. Chem., Int. Ed.*, 2004, **43**, 6596–6616.
8 E. T. Kool, *Chem. Rev.*, 1997, **97**, 1473–1488.
9 D. W. Bolen and G. D. Rose, *Annu. Rev. Biochem.*, 2008, **77**, 339–362.
10 D.-W. Zhang, X. Zhao, J.-L. Hou and Z.-T. Li, *Chem. Rev.*, 2012, **112**(10), 5271–5316.
11 L. Brunsveld, B. J. B. Folmer, E. W. Meijer and R. P. Sijbesma, *Chem. Rev.*, 2001, **101**, 4071–4098.
12 D. L. Cameron, J. Jakus, S. R. Pauleta, G. W. Pettigrew and A. Cooper, *J. Phys. Chem. B*, 2010, **114**, 16228–16235.
13 J. L. Cook, C. A. Hunter, C. M. R. Low, A. Perez-Velasco and J. G. Vinter, *Angew. Chem., Int. Ed.*, 2007, **46**, 3706–3709.
14 R. Cabot and C. A. Hunter, *Chem. Soc. Rev.*, 2012, **41**, 3485–3492.
15 S. L. Cockroft and C. A. Hunter, *Chem. Commun.*, 2006, 3806–3808.
16 S. L. Cockroft and C. A. Hunter, *Chem. Commun.*, 2009, 3961–3963.
17 L. F. Newcomb and S. H. Gellman, *J. Am. Chem. Soc.*, 1994, **116**, 4993–4994.
18 M. Ōki, *Acc. Chem. Res.*, 1990, **23**, 351–356.
19 S. Paliwal, S. Geib and C. S. Wilcox, *J. Am. Chem. Soc.*, 1994, **116**, 4497–4498.
20 E.-i. Kim, S. Paliwal and C. S. Wilcox, *J. Am. Chem. Soc.*, 1998, **120**, 11192–11193.
21 I. K. Mati and S. L. Cockroft, *Chem. Soc. Rev.*, 2010, **39**, 4195–4205.
22 K. B. Muchowska, C. Adam, I. K. Mati and S. L. Cockroft, *J. Am. Chem. Soc.*, 2013, **135**, 9976–9979.
23 F. R. Fischer, W. B. Schweizer and F. Diederich, *Chem. Commun.*, 2008, 4031–4033.
24 A. E. Aliev, J. Moise, W. B. Motherwell, M. Nic, D. Courtier-Murias and D. A. Tocher, *Phys. Chem. Chem. Phys.*, 2009, **11**, 97–100.
25 B. Bhayana and C. S. Wilcox, *Angew. Chem., Int. Ed.*, 2007, **46**, 6833–6836.
26 W. R. Carroll, P. Pellechia and K. D. Shimizu, *Org. Lett.*, 2008, **10**, 3547–3550.
27 B. W. Gung and J. C. Amicangelo, *J. Org. Chem.*, 2006, **71**, 9261–9270.
28 B. W. Gung, X. Xue and Y. Zou, *J. Org. Chem.*, 2007, **72**, 2469–2475.
29 F. Cozzi and J. S. Siegel, *Pure Appl. Chem.*, 1995, **67**, 683–689.
30 R. Annunziata, M. Benaglia, F. Cozzi and A. Mazzanti, *Chem.–Eur. J.*, 2009, **15**, 4373–4381.
31 W. B. Motherwell, J. Moise, A. E. Aliev, M. Nic, S. J. Coles, P. N. Horton, M. B. Hursthouse, G. Chessari, C. A. Hunter and J. G. Vinter, *Angew. Chem., Int. Ed.*, 2007, **46**, 7823–7826.
32 F. R. Fischer, P. A. Wood, F. H. Allen and F. Diederich, *Proc. Natl. Acad. Sci. U. S. A.*, 2008, **105**, 17290–17294.
33 F. R. Fischer, W. B. Schweizer and F. Diederich, *Angew. Chem., Int. Ed.*, 2007, **46**, 8270–8273.
34 F. Hof, D. M. Scofield, W. B. Schweizer and F. Diederich, *Angew. Chem., Int. Ed.*, 2004, **43**, 5056–5059.
35 C. Zhao, R. M. Parrish, M. D. Smith, P. J. Pellechia, C. D. Sherrill and K. D. Shimizu, *J. Am. Chem. Soc.*, 2012, **134**, 14306–14309.
36 C. A. Hunter, *Angew. Chem., Int. Ed.*, 2004, **43**, 5310–5324.
37 C. A. Hunter and H. L. Anderson, *Angew. Chem., Int. Ed.*, 2009, **48**, 7488–7499.
38 J. L. Cook, C. A. Hunter, C. M. R. Low, A. Perez-Velasco and J. G. Vinter, *Angew. Chem., Int. Ed.*, 2008, **47**, 6275–6277.

Published on 23 July 2013. Downloaded by Michigan State University on 21/01/2016 19:52:01.

39 The inclusion of a solvophobic term ($\Delta\alpha_s\beta_s$) did not significantly improve the quality of the fitting, consistent with the fact that the O- and H-conformers have very similar solvent-accessible areas (Fig. S5–S11†).
40 Z. Yin, L. Jiang, J. He and J.-P. Cheng, *Chem. Commun.*, 2003, 2326–2327.
41 K. J. Kamer, A. Choudhary and R. T. Raines, *J. Org. Chem.*, 2012, **78**, 2099–2103.
42 C. A. Hunter, *Chem. Sci.*, 2013, **4**, 1687–1700.

This journal is © The Royal Society of Chemistry 2013